PHILOSOPHICAL TRANSACTIONS OF THE ROYAL SOCIETY A

Phil. Trans. R. Soc. A (2010) **368**, 2123–2139
doi:10.1098/rsta.2010.0015

Biologically active collagen-based scaffolds: advances in processing and characterization

By I. V. Yannas[1,2,*], D. S. Tzeranis[1], B. A. Harley[3] and P. T. C. So[1,2]

[1]*Department of Mechanical Engineering, and* [2] *Department of Biological Engineering, Massachusetts Institute of Technology (MIT), Cambridge, MA 02139, USA*

[3]*Department of Chemical and Biomolecular Engineering, University of Illinois at Urbana-Champaign, Urbana, IL 61801, USA*

A small number of type I collagen–glycosaminoglycan scaffolds (collagen–GAG scaffolds; CGSs) have unusual biological activity consisting primarily in inducing partial regeneration of organs in the adult mammal. Two of these are currently in use in a variety of clinical settings. CGSs appear to induce regeneration by blocking the adult healing response, following trauma, consisting of wound contraction and scar formation. Several structural determinants of biological activity have been identified, including ligands for binding of fibroblasts to the collagen surface, the mean pore size (which affects ligand density) and the degradation rate (which affects the duration of the wound contraction-blocking activity by the scaffold). Processing variables that affect these determinants include the kinetics of swelling of collagen fibres in acetic acid, freezing of the collagen–GAG suspension and cross-linking of the freeze-dried scaffold. Recent developments in the processing of CGSs include fabrication of scaffolds that are paucidisperse in pore size, scaffolds with gradients in physicochemical properties (and therefore biological activity) and scaffolds that incorporate a mineral component. Advances in the characterization of the pore structure of CGSs have been made using confocal and nonlinear optical microscopy (NLOM). The mechanical behaviour of CGSs, as well as the resistance to degradative enzymes, have been studied. Following seeding with cells (typically fibroblasts), contractile forces in the range 26–450 nN per cell are generated by the cells, leading to buckling of scaffold struts. Ongoing studies of cell-seeded CGSs with NLOM have shown an advantage over the use of confocal microscopy due to the ability of the former method to image the CGS surfaces without staining (which alters its surface ligands), reduced cell photodamage, reduced fluorophore photobleaching and the ability to image deeper inside the scaffold.

Keywords: collagen–GAG scaffolds; organ regeneration; biologically active scaffolds; scaffold processing; nonlinear optical microscopy

*Author for correspondence (yannas@mit.edu).

One contribution of 14 to a Theme Issue ‘Advanced processing of biomaterials’.

1. Introduction

The use of scaffolds in tissue engineering and regenerative medicine has been increasing quite rapidly, as shown by the number of publications dealing with the topic and by the number of clinical cases in which the treatment centres on devices based on scaffolds. Of these, certain collagen-based scaffolds have shown by far the greatest promise. A special class of scaffolds are analogous to the extracellular matrix (ECM). They are synthesized as graft copolymers of type I collagen and a glycosaminoglycan (GAG), and have particularly attracted the attention of investigators due to their rapidly increasing use in clinical settings.

Detailed methodologies for synthesis and characterization of collagen-based scaffolds have been published. Nevertheless, both processing and characterization methods are evolving. This review focuses on recent developments in these two areas. In order to appreciate the often critical importance of certain processing parameters and the need for adequate methods of characterization for these biologically active materials, we will first summarize two current areas of research. First, we will describe briefly the clinical experience with collagen–GAG scaffolds (CGSs); and second, we will summarize the available information on the structural features (structural determinants) that are responsible for their unusual biological activity.

2. Clinical experiences with collagen–glycosaminoglycan scaffolds

There is accumulating evidence that the healing process of an injured organ in the adult mammal can be modified to yield a partly or wholly regenerated organ. In almost all such processes, the critical 'reactant' supplied by the investigators was a scaffold synthesized as an ECM analogue, occasionally seeded with autologous epithelial cells of the organ being regenerated. The most extensive data on induced organ regeneration are available with skin and peripheral nerves (see review in Yannas 2001). Data with other organs from the work of several investigators were presented in a recent volume (Yannas 2005*a*). We review the evidence very briefly below.

(*a*) *Regeneration of skin*

A detailed example of induced skin regeneration, originally described as 'artificial skin', has been described elsewhere (Yannas *et al.* 1981, 1982, 1989; Murphy *et al.* 1990; Compton *et al.* 1998; Orgill & Yannas 1998). The data describe the structural and functional similarities and differences among normal skin, scar and regenerated skin in the adult guinea pig and the swine following grafting of dermis-free defects with the keratinocyte-seeded dermis regeneration template (DRT). This scaffold has unusual regenerative activity. The DRT is a macromolecular network synthesized as a highly porous analogue of the ECM, with highly specific structure that degrades *in vivo* at a controlled rate. Among other characteristics, regenerated skin is mechanically competent, fully vascularized and sensitive to touch as well as heat or cold. The regenerated dermal–epidermal junction, with its extensive formations of rete ridges and

capillary loops, leaves no doubt that de novo regenerated skin organ is clearly not a scar. However, regenerated skin differs from physiological skin in the absence of skin appendages (hair follicles, sweat glands, etc.).

Seeding of the template with keratinocytes leads to *simultaneous* regeneration of a dermis and an epidermis (Yannas *et al.* 1981, 1982, 1989), while omission of seeded cells leads to *sequential* regeneration of the dermis and epidermis. The simultaneous process leads to a clinically desirable result within about two to three weeks, but is complicated by the need to prepare the seeded template in a clinical setting. The sequential process is obviously simpler to implement clinically. Following grafting, the template induces regeneration of the dermis, and the new dermis is spontaneously epithelialized from the wound margin. Rather than wait for re-epithelialization in the clinical setting, a thin autoepidermal graft is preferably applied on the newly synthesized dermis (Burke *et al.* 1981; Heimbach *et al.* 1988; Fang *et al.* 2002).

(*b*) *Regeneration of adult organs other than skin*

In addition to skin, confirmed observations of at least partial regeneration using scaffolds with high biological activity (templates) have also been reported with peripheral nerves (Chamberlain *et al.* 1998; Zhang & Yannas 2005) and the conjunctiva (Hsu *et al.* 2000). Significant progress in the study of regeneration has been recently reported independently in studies of bone (Mistry & Mikos 2005), heart valves (Rabkin-Aikawa *et al.* 2005), articular cartilage (Kinner *et al.* 2005), urological organs (Atala 2005) and the spinal cord (Verma & Fawcett 2005). The reader is also referred to a volume with reviews (Yannas 2005*a*).

(*c*) *Established clinical uses*

Two collagen-based scaffolds, approved by the Food and Drug Administration for use with patients who lacked sufficient skin (Integra) or those whose limb was paralysed due to severe trauma (Neuragen), have been used clinically. By 2008, the first device had been used with over 100 000 patients who were severely burned, or were undergoing plastic surgery of the skin or suffered from chronic skin wounds. Clinical use of these devices, especially the first, appears to be steadily increasing in clinics around the world (e.g. Katrana *et al.* 2008; Sasidaran *et al.* 2008; Wakabayashi *et al.* 2008; Baldwin *et al.* 2009).

(*d*) *Limitations of collagen–glycosaminoglycan scaffolds as regenerative devices*

These devices do not induce regeneration of entirely normal organs. As mentioned earlier, skin regenerated by the use of CGSs lacks appendages and becomes vascularized within several days. This rate would have to be accelerated in order to improve significantly the infection-preventing function of the graft. Peripheral nerves that were induced to regenerate with collagen-based scaffolds in the form of tubes conduct electric impulses that are somewhat slower and significantly weaker in amplitude than observed with normal nerves (although scaffolds that have been recently synthesized, but are not commercially available, improve significantly on the clinically available device).

3. Structural determinants of biological activity

A distinctive characteristic of certain collagen-based scaffolds is their biological activity. A few highly porous scaffolds with distinctive structure bind contractile fibroblasts on their extensive surface via integrin–ligand binding and, in doing so, block the generation of macroscopic contractile forces that are normally deployed to contract wounds in injured organs. Blocking of contraction appears to be required for the regeneration of adult tissues at the site of injury. This finding that certain solid surfaces possess such an activity often surprises investigators who have commonly associated biological activity with soluble macromolecules, such as enzymes, rather than with insoluble surfaces. Indeed, textbooks of biochemistry typically deal with interactions of cells with isolated macromolecules in a sea of buffer, rather than describing cells interacting with a solid-like medium. These perceptions are changing following the successful use of scaffolds in the treatment of several patient populations.

The locus of biological activity of scaffolds can be specified using the concept of structural determinants. Although determinants appear to have been identified so far only for collagen-based scaffolds, it is already becoming clear that they transcend the classical molecular features, such as functional groups with specific conformation, as is common with enzymes, antibodies, etc. For example, it is now clear that the average pore diameter is a powerful determinant of the biological activity of a scaffold.

In studies of the regenerative activity of scaffolds, it is very useful to draw on a theoretical base for the economic description of the observed phenomena. There is considerable evidence from many sources (reviewed in Yannas 2001, 2005*c*) that the induction of organ regeneration requires two steps, together amounting to suitable blocking of the adult healing response to tissue injury. The first step is blocking of wound contraction. There is also evidence of a second step, namely the presence of a scaffold over a maximum duration, while the scaffold acts as a topological template for synthesis of new stroma that is architecturally appropriate for the organ being studied. Assays for regenerative activity have been accordingly based on this two-tiered mechanism, especially the first one, which principally involves blocking of wound contraction in the injured organ.

The structural determinants of scaffold activity have been largely identified (Yannas 2001, 2005*c*) and are summarized in table 1. Consistently with the contraction-blocking mechanism described earlier, it has been postulated that the regenerative activity of a scaffold amounts, to a large extent, to a capacity for binding on its surface most of the contractile cells in the wound. Based on immunohistochemical evidence (Yannas 2005*b*,*c*), it appears that such extensive binding denies these cells the opportunity to induce contraction of the wound bed.

Structural features that control cell–scaffold binding include the chemical identity of the ligands, the pore size and the duration of the scaffold in undegraded form (table 1). The term ligand is used in this text to describe the specific amino acid motifs in the proteins found on the scaffold surface, where cell adhesion molecules bind. For the cell–CGS system, the main protein of interest is collagen, and the major cell adhesion molecules of interest are collagen-binding integrins, mainly integrins $\alpha1\beta1$ and $\alpha2\beta1$. The chemical identity of the ligand is crucial for specific binding of cells mainly via integrins $\alpha1\beta1$ and $\alpha2\beta1$ that are known to be used in wound contraction (see below). The absence of ligands of the appropriate

Table 1. Structural determinants of regenerative activity of two CGSs.

structural parameter required for regenerative activity	skin regeneration[a]	nerve regeneration[b]	structural feature hypothetically responsible for contraction blocking
type I collagen/GAG (w/w)	98/2	98/2	ligand identity
residual collagen fibre banding	approximately 5% of native collagen	approximately 5% of native collagen	reduction in recruitment of contractile cells
average molecular weight between cross-links (kDa)	5–15	40–60	controls duration of undegraded scaffold during contraction
average pore diameter (μm)	20–120	5–10	ligand density
pore-channel orientation	random	axial	ligand orientation

[a]Approximate levels of structural determinants observed in skin regeneration studies conducted by grafting the scaffold on a full-thickness skin wound (Yannas *et al.* 1989).
[b]Approximate levels of structural determinants observed in peripheral nerve regeneration studies performed by inserting the scaffold inside a nerve conduit (the conduit connected the two stumps of the transected nerve across an experimental gap of defined length) (Chang *et al.* 1990; Chang & Yannas 1992).

chemical identity (e.g. the hexapeptide motif GFOGER found in collagen; Knight *et al.* 2000) should delete the specific cell-binding activity of the scaffold. This may explain the finding that, although cells bind non-specifically on the surface of synthetic polymers, the latter do not appear to show regenerative activity.

The pore size of the scaffold controls the specific surface available for binding (specific surface increases with decreasing pore size). The pore size, therefore, controls the density of ligands for cell receptors that are present on the surface of the scaffold. When the pore size becomes much larger than 50–100 μm, the regenerative activity falters and eventually is not observed. Loss of ability to bind a minimum number of cells residing in the wound bed, leading to inability to control contraction, may therefore explain the upper limit of the pore size. An alternative explanation focuses on the dimensionality of cell binding on the scaffold surface as a variable that affects the phenotype of the bound cells. It is suggested that cells inside small enough pore channels (much smaller, say, than 200 μm) bind over their entire surface (three-dimensional binding) and possess a different phenotype than do cells inside much larger pores that provide lower opportunities for cell binding around the cell surface, leading to two-dimensional binding. The dimensionality of cell binding has been implicated in many recent studies as a determinant of cell phenotype (e.g. Even-Ram & Yamada 2005; Meshel *et al.* 2005). At the other extreme of pore size, the regenerative activity is lost when the pore size is much smaller than 10 μm. In this case, it has been observed that cells cannot penetrate into the scaffold and eventually bind on its extensive interior surface (table 1).

The duration of the scaffold is the length of time required for the scaffold to remain in a relatively solid-like form. The requirement calls for an optimal duration. A requirement for a minimal duration limit may hypothetically stem

from the need for the presence of an insoluble cell-binding surface over at least the entire period (approximately three weeks), during which contraction remains active during wound healing. Scaffold degradation that occurs too early apparently prevents the solubilized scaffolds from binding contractile cells during the entire contractile period; contraction is, therefore, not blocked. It is not clear what is the minimal particle size for a partly degraded scaffold below which cell binding is cancelled. A hypothetical model calls for a minimal average particle size that is lower than the average pore size, leading to loss of three-dimensional binding that may putatively be required for effective binding (see above).

Independent of its cell-binding activity, the collagen-based scaffold with regenerative activity appears to interfere with wound contraction via an additional pathway. CGSs that were prepared by selective melting of collagen banding periodicity (without affecting the native triple helical structure of collagen) have been shown to downregulate the well-known process of platelet aggregation on collagen surfaces (Sylvester *et al.* 1989). During wound healing, platelet binding normally leads, via platelet degranulation, to a release of several inflammatory cytokines, including platelet-derived growth factor and transforming growth factor β1 (TGFβ1). Inhibition of platelet binding on the surface of the grafted scaffold is expected to lead to blocking the release of inflammatory cytokines in the wound bed, resulting in diminished concentrations of the normal drivers of wound contraction. Downregulation of TGFβ1 concentration in the wound bed is particularly important since this cytokine has been involved in the differentiation of fibroblasts to myofibroblasts (Desmouliere *et al.* 2005). Downregulation of TGFβ1 by a factor of three in the presence of an active scaffold, relative to the presence of an inactive scaffold, has in fact been observed *in vivo*. This observation may explain the finding that the density of myofibroblasts in scaffold-grafted wounds is a relatively small fraction (about 20%) of their density in the absence of any scaffold (Murphy *et al.* 1990) or even in the presence of an inactive scaffold (Yannas 2001).

An active scaffold blocks contraction, therefore, by two apparently independent mechanisms: first, by binding contractile cells, thereby downregulating their ability to exert macroscopic contractile forces that close the wound; and second, by reducing significantly the number of contractile cells available to participate in contraction.

Consideration of the second major step in a regenerative process, namely the synthesis of a stroma with the appropriate architecture, may explain the remainder of the observations about structural determinants in table 1. Although scaffold insolubility is required during the process of contraction (see above), persistent scaffold insolubility beyond termination of the contraction process interferes sterically with the synthesis of new stroma. The requirement for a critical scaffold-duration period, with a minimum and maximum, is thereby explained (Yannas 2001). Further, synthesis of a stroma with suitable architecture often requires preferential collagen-fibre deposition along certain directions. For example, synthesis of a stroma for a peripheral nerve regeneration requires oriented synthesis along the direction of the nerve fibres. This requirement may explain the observation for an axial orientation of scaffold struts during nerve regeneration while regeneration of a dermis, a random array of collagen fibres, is associated with a strut arrangement that lacks orientation (table 1).

The molecular events that characterize binding of contractile cells on a scaffold surface are a subject of increasing interest. The expression of contractile phenotypes in fibroblasts during wound healing resembles a positive feedback loop: cells apply forces to their environment, remodel the ECM and, at the same time, create strong focal adhesions that allow them to apply even larger contraction forces (Hinz 2006). A requirement for the development of such a positive feedback loop is the ability of contractile cells to bind strongly to their environment, which depends on the type and density of available ligands for their adhesion molecules. Since the control of the contractile phenotype of fibroblasts is an important requirement in regenerative medicine (Yannas 2005*b*,*c*), it is necessary to focus attention on cell binding to the surrounding matrix and how this is affected by the presence of a CGS. Adhesion of cells to collagen-rich stroma is mediated through the collagen-binding class of integrins (α1β1, α2β1, α10β1 and α11β1; see Hynes 2002). Each one of these four integrins binds multiple types of collagen (e.g. types I, II, III and IV) or other ECM molecules, at multiple ligands, with various affinities (Tuckwell *et al.* 1995; Calderwood *et al.* 1997; Knight *et al.* 2000; Tulla *et al.* 2001; Kim *et al.* 2005). Among the collagen-binding integrins, α1β1 and α2β1 are the most widely expressed and well studied. Indeed, integrins α1β1 and α2β1 have been shown to dominate binding of fibroblasts to collagen surfaces during the contraction process (Racine-Samson *et al.* 1997) and binding of pancreatic cancer cells in CGSs (Grzesiak & Bouvet 2007). Studies of integrin-mediated cell adhesion in CGSs are under way in many laboratories.

4. Effects of processing variables on biological activity

The preceding discussion leads directly to a discussion of processing variables that need to be controlled carefully in order to synthesize collagen-based scaffolds with the desired biological activity. In this section, we discuss several critical points along the scaffold fabrication process at which loss of control leads to loss of activity. A detailed discussion of the processing steps leading to active scaffolds in a laboratory setting has been published (Chamberlain *et al.* 1998). Manufacturing plants that produce collagen-based scaffolds on an industrial scale have been operated since 1993 (Integra LifeSciences Corp., Plainsboro, NJ, USA).

The process consists of a few steps that are listed below with very brief commentary on the consequences of loss of control at the physicochemical level.

Type I collagen in microparticulate form, extracted from hide or tendon or other sources, is swollen in 0.05 M acetic acid over a period necessary to selectively melt out the banding without affecting the triple helical structure. Inadequate exposure to acetic acid, a good collagen solvent, at this point, leads to incomplete loss of banding with consequent deleterious increase in platelet aggregation on the surface of the scaffold. Problems can arise either due to insufficient acid or insufficient time of exposure. Loss of control of the mass of collagen added leads to inadequate control of the pore volume fraction, which affects the degradation rate.

The suspension of collagen fibrils is precipitated out with the addition of a sulphated GAG, such as chondroitin 6-sulphate. Precipitation occurs by complexation of the two polymers. Addition of an insufficient mass of GAG leads to loss of a substantial fraction of the resistance to degradation of the scaffold.

The collagen–GAG suspension is frozen at a rate that determines not only the average pore size (lower freezing rates lead to higher pore sizes) but also the uniformity of the pore size. Control of freezing is an essential step in the preparation of scaffolds with the appropriate pore size. The potential contribution of pore-size uniformity to biological activity has not been explicitly determined. At the end of the freeze-drying step, the moisture content of the scaffold is in the range 5–8 wt%.

Following drying, the highly porous scaffold is frequently cross-linked by a two-step process. The first step is a dehydrothermal treatment, which does not require use of a cross-linking agent. In this process, the scaffold is exposed to temperatures of 100–120°C under high vacuum. This step leads to dehydration of the scaffold to a level below about 2 wt%. Drastic dehydration is required for self-cross-linking of collagen by the formation of amide bonds between protein chains and probably also by the formation of collagen–GAG bonds. Gelatinization, or melting of the triple helical structure of collagen, occurs if the moisture content at the beginning of the heating process is high enough to induce melting of the triple helical structure at the dehydration temperature. In addition to the loss of specific ligands for cell binding, gelatin degrades *in vivo* at a very highly accelerated rate. Additional cross-linking is frequently desired and is supplied using a cross-linking agent. Insufficient control of cross-linking conditions leads to loss of the optimal *in vivo* duration of the scaffold.

Finally, during handling, a highly porous scaffold (pore volume fraction typically 99.5%) loses its activity after being exposed to a highly humid atmosphere followed by exposure to a relatively dry one. This exposure leads to strong humidification of the scaffold, followed by closure of pores during drying due to the action of capillary forces.

5. Recent developments in processing of scaffolds

CGSs are fabricated by a lyophilization (freeze-drying) process (Yannas *et al.* 1989). The freezing step creates an interconnected network of ice crystals surrounded by an amorphous collagen–GAG phase. Ice is removed by sublimation, resulting in the formation of a porous CGS sheet, which is subsequently cross-linked by thermal or chemical methods. If the freezing step is not controlled appropriately, the pores that form are highly polydisperse in diameter. Proper selection of the heat-transfer parameters during the freezing step has reduced the pore-size polydispersity significantly (O'Brien *et al.* 2004). Control of cooling of the lyophilizer shelves at an intermediate constant rate, instead of quenching, and ensuring that the mould makes good contact with the shelf are the two steps that result in the fabrication of CGS sheets of uniform structural properties throughout their volume. Using this new technique, the resulting CGS pores show less dispersity, are well interconnected and highly equiaxed.

Another recently developed technique leads to the fabrication of CGS tubes that are characterized by radial orientation of pores (Harley *et al.* 2006). The technique relies on simultaneous sedimentation and freezing of a collagen–GAG suspension to create tubular scaffolds with a pore size that varies along the radial direction. In one version, the mean pore size at the inner part of the

tube is approximately 20 μm or higher, whereas at the outer part of the tube, the mean pore size is approximately 5 μm or lower. Relatively large pore sizes are expected to encourage cell migration, whereas very low pore sizes exclude cells but allow diffusion of macromolecules. A large variety of gradient scaffolds have been described in the patent literature (Yannas *et al.* 2006).

The incorporation of new chemical components in CGSs can lead to new biomaterials and promising applications in regenerative medicine. The addition of calcium phosphate in the standard collagen–GAG fabrication protocol leads to scaffolds of controllable mineral : organic component ratios (up to 0.08) and pore-size distribution (Kanungo *et al.* 2008; Harley *et al.* 2009*a*,*b*; Lynn *et al.* 2009). The chemical and pore-structural composition of these mineralized scaffolds mimic the properties found in bone tissue. Furthermore, new methods for the fabrication of multi-phase scaffolds with compartments of distinct chemical composition enable the fabrication of scaffolds that consist of a mineralized part and an organic (collagen–GAG) part. A 'liquid-phase co-synthesis' method enables joining the two parts without any hard interfaces. Such multi-phase scaffolds could potentially be used in orthopaedic tissue-engineering applications, for example, in the repair of joints (Harley *et al.* 2009*a*, 2010).

6. Advances in structural and functional characterization of collagen–glycosaminoglycan scaffolds

The structural properties of the highly porous CGS (strut dimensions and pore-size distribution) have been previously quantified using scanning electron microscopy images. Alternatively, the pore-size distribution of a scaffold can be obtained by analysing images of thin sections of paraffin-embedded CGSs obtained by optical microscopy. Processing of such images using the Scion Image software package (Scion Corporation, Frederick, MD, USA) was used to quantify the pore-size distribution of the CGS fabricated by the freezing process based on the constant cooling rate that was described above (O'Brien *et al.* 2004). In the same study, microcomputed tomography imaging was also applied to measure the scaffold pore size and verify the results obtained by histology.

A less invasive method to quantify the structural properties of CGSs involves processing of three-dimensional images of the scaffolds. Three-dimensional images can be acquired by confocal (Harley *et al.* 2008) or nonlinear optical microscopy (NLOM) (So *et al.* 2000). Confocal microscopy requires fluorescence staining of collagen, which may affect cell–matrix interactions because staining can change the density of ligands on the surface of scaffold struts. NLOM makes use of the endogenous second-harmonic emission of collagen to visualize CGSs without staining (Campagnola & Loew 2003). The second-harmonic emission generated by collagen in CGS struts is not particularly strong compared with the emission generated by collagen fibrils in tissues. This is probably due to partial loss of collagen banding (required for prevention of platelet aggregation, Yannas 1990) that occurs during swelling in acetic acid, a step in the CGS fabrication process. The presence of banding in native collagen fibrils is expected to amplify the second-harmonic emission owing to the coherence character of the phenomenon (Campagnola & Loew 2003).

The mechanical properties of CGSs have been recently characterized at the macroscopic and microscopic levels (Harley *et al.* 2007*a*). Unidirectional, unconfined compression and tension tests performed on dry or hydrated CGS samples showed stress–strain behaviour that is characteristic of low-density open-cell foam materials. Young's moduli in the linear elastic regime (up to 5% strain) of the stress–strain curve of dry and hydrated CGSs were equal to $E_{\mathrm{CGS}} = 30\,\mathrm{kPa}$ and $E_{\mathrm{CGS}} = 208\,\mathrm{Pa}$, respectively, and did not depend on the pore size. Young's modulus of the individual struts in a dry CGS was measured by atomic force microscopy (AFM), yielding $E_{\mathrm{strut}} = 762\,\mathrm{MPa}$. Cellular solids theory was used to model the mechanical properties of CGS as a function of the normalized scaffold density $\rho_{\mathrm{CGS}}/\rho_{\mathrm{strut}}$, where ρ_{CGS} is the scaffold density and ρ_{strut} is the strut density. For the CGSs discussed in this article, the ratio $\rho_{\mathrm{CGS}}/\rho_{\mathrm{strut}}$ takes values in the range 0.0058–0.018. CGSs were found to be significantly stiffer in tension in the plane of the CGS sheet due to a thin (approx. 200 μm thick) layer of higher density that typically forms at the top surface of the CGS sheet during freeze drying. Thermal (dehydrothermal) and chemical cross-linking (treatment with 1-ethyl-3-carbodiimide hydrochloride (EDAC) and *N*-hydroxysuccinimide (NHS)) had a significant effect on the scaffold stiffness (E_{CGS} increased 40% following dehydrothermal (DHT) and up to 10-fold by EDAC/NHS cross-linking, respectively) due to cross-links that are formed inside the CGS struts, without affecting the pore structure (Pek *et al.* 2004; Harley *et al.* 2007*a*).

Chemical characterization and modification of CGSs have been pursued during the past few years. The chemical properties of the CGS affect scaffold stiffness, degradation rate and the ability of cells to bind and interact with the CGS. As described earlier, CGSs are fabricated from collagen I and chondroitin 6-sulphate (a GAG) and are cross-linked by thermal (DHT) or chemical treatment (EDAC/NHS). A recent *in vitro* study showed that collagenase can digest uncross-linked CGSs or CGSs cross-linked by the DHT method, but could not digest chemically cross-linked CGSs, suggesting that chemical cross-linking inhibits CGS remodelling by collagenase (Pek *et al.* 2004). The same study indicated that the effect of chondroitinase on the GAG content of DHT cross-linked scaffolds was significant, while its effect on the GAG content of chemically cross-linked scaffolds was small, suggesting that chemical cross-linking is based on the formation both of collagen–collagen and collagen–GAG bonds, as postulated earlier for cross-linking based on DHT or use of aldehydes (Yannas *et al.* 1980).

7. Characterization of cell–scaffold interactions

Studies of cell–scaffold systems provide information on the biological activity of CGSs that cannot be obtained otherwise. CGSs provide useful *in vitro* experimental platforms for studying how cell–matrix interactions affect various cell phenotypes of interest, such as contraction, differentiation, adhesion and migration. Cell contraction is a phenotype of particular interest in regenerative medicine (Yannas 2001, 2005*a*,*b*,*c*).

In several studies, an attempt was made to estimate the magnitude of the contractile forces applied by fibroblasts seeded in CGSs. Soon after seeding a CGS with fibroblasts, cells adhere to the surrounding struts and apply contractile forces

that shrink the CGS sample. The resulting macroscopic force was measured by a force transducer attached to a clamped cell-seeded CGS specimen (Freyman *et al.* 2001). The time response of the contractile force increased exponentially with a characteristic time constant of approximately 5 h. A mean contractile force of 1 nN per cell was obtained by normalizing the measured asymptotic force with the total number of cells seeded in the CGS. This force estimate was observed to be independent of the cell density in the CGS, and represents a lower bound on the magnitude of the contractile force per cell since it does not consider the random orientation of cells inside the CGS. A direct estimation of the contractile force applied by individual fibroblasts inside the CGS was based on the observation that usually cells can buckle the struts to which they bind. The contractile force applied by a single cell was estimated using column buckling theory with geometric and stiffness properties obtained from microscopy images and AFM measurements of single CGS struts, respectively (Harley *et al.* 2007*b*). The mean contractile force applied by each cell was estimated at 26 nN, and an upper bound of 450 nN was reported based on the inability of cells to buckle large-diameter struts.

The adhesion of fibroblasts to a CGS depends on both the structure and the surface chemistry of the CGS. Using a standard cell adhesion assay, it was shown that the fraction of fibroblasts that adhere to a CGS within a certain time window is analogous to the CGS-specific surface area or, equivalently, inversely proportional to the CGS pore size (O'Brien *et al.* 2005).

Although the molecular mechanisms of cell chemotaxis and migration on flat cell culture dishes are quite well understood (Ridley *et al.* 2003), it has been found that cells inside three-dimensional environments express unique mechanisms related, among others, to adhesion and cell migration (Even-Ram & Yamada 2005; Meshel *et al.* 2005). CGSs provide useful *in vitro* systems for studies of molecular aspects of cell migration in three-dimensional micro-environments that resemble much closer those in the native ECM of tissues (e.g. Park *et al.* 2007; Timmins *et al.* 2007). For example, the expression of $\alpha 2\beta 1$ and $\alpha 1\beta 1$ integrins in pancreatic cancer cells was studied inside the three-dimensional micro-environment provided by a typical CGS (Grzesiak & Bouvet 2007). In another study, time-lapsed confocal microscopy was used to quantify kinematic characteristics of fibroblast migration (velocity, persistence and directionality) inside CGSs and their correlation with CGS structure (Harley *et al.* 2008). The average speed of fibroblasts (ranging from 2 to 20 $\mu m\,h^{-1}$) was shown to be inversely proportional to the CGS mean pore size. This was explained by the observation that cells move faster on strut junctions, possibly due to the larger number of ligands available locally for binding. The same study also reports a biphasic dependence of cell speed on the CGS stiffness, a result previously reported on cell migration in two- and three-dimensional environments.

Scaffold analogues of ECM are expected to stimulate cells in a different, and yet unknown, way compared with the stimulation of cells cultured on standard plastic flat culture dishes (Yamada & Cukierman 2007). In order to quantify how gene expression is affected by the micro-environment that cells sense in a CGS, oligonucleotide micro-arrays were used to compare mRNA expression in cells cultured in CGSs versus cells cultured on standard cell culture dishes (Klapperich & Bertozzi 2004; Jaworski & Klapperich 2006). These studies showed

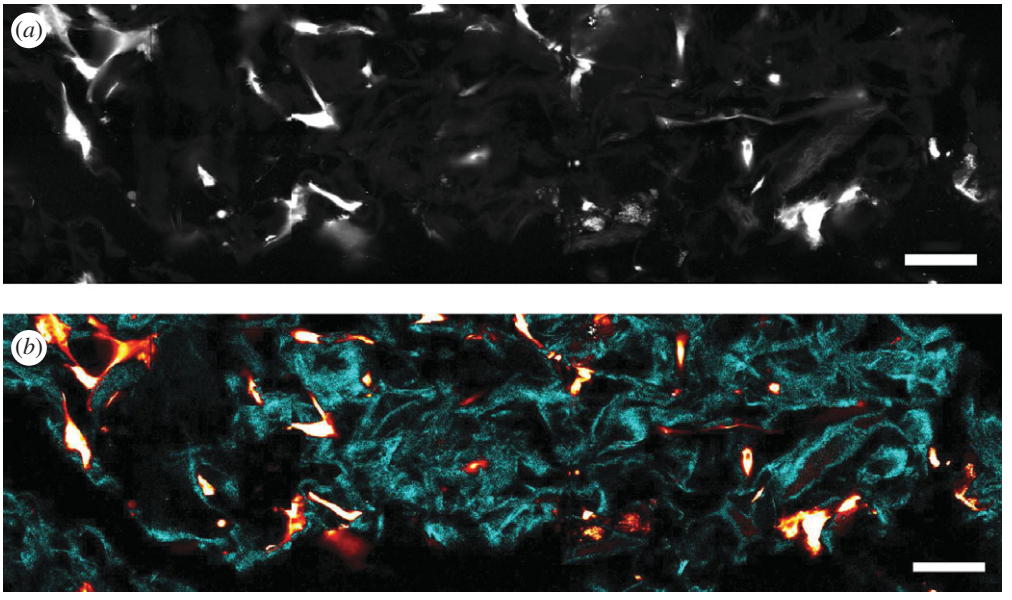

Figure 1. Image of a fibroblast-seeded CGS acquired by NLOM. The cells (human dermal fibroblasts) are labelled using Calcein acetoxymethyl (AM) cell-tracking dye. (*a*) Raw intensity image acquired by the microscope sensor. (*b*) Estimation of cell (red–white) and CGS strut (blue) objects. The estimation is based on the detected emission spectrum at each pixel and the known emission spectra of collagen and calcein AM dye. Scale bars, (*a*,*b*) 40 µm.

that the three-dimensional micro-environment (and not simply the presence of collagen and GAG) inside the CGS upregulates several genes in cells that are related to matrix remodelling and angiogenesis.

Imaging of cell–matrix interactions inside CGSs appears to be on the verge of a revolution in methodology following the increasing use of NLOM (Zipfel *et al.* 2003). Examples appear in figures 1 and 2. The two major phenomena used with NLOM are two-photon excitation fluorescence (TPEF) and second-harmonic generation (SHG). In TPEF, a fluorescent molecule is excited by the near-simultaneous absorption of two photons of wavelength λ_{ex}. Within a few nanoseconds, a typical fluorophore returns to its ground state and emits a photon of wavelength $\lambda_{em} > \lambda_{ex}/2$ (Denk *et al.* 1990). In contrast, in ordinary fluorescence imaging, the fluorophore absorbs a single photon (λ_{ex}) and emits a single photon of lower energy ($\lambda_{em} > \lambda_{ex}$). In SHG, arrays of biomolecules, lacking centrosymmetry, scatter light at wavelength $\lambda_{scat} = \lambda_{ex}/2$ upon illumination (Campagnola & Loew 2003). The magnitude of TPEF and SHG emission depends nonlinearly on the magnitude of the excitation light. This is used in NLOM to achieve three-dimensional imaging, as follows. When a pulsed laser is focused on the biological sample, the illumination intensity is large enough to create detectable emission only inside a small volume around the focus. TPEF is emitted by intrinsic fluorophores found in cells or tissues (e.g. reduced nicotinamide adenine dinucleotide, riboflavin and elastin), by proteins fused genetically to fluorescent proteins or by fluorescent stains added externally. SHG has been observed from originates from arrays of several proteins such as collagen and myosin.

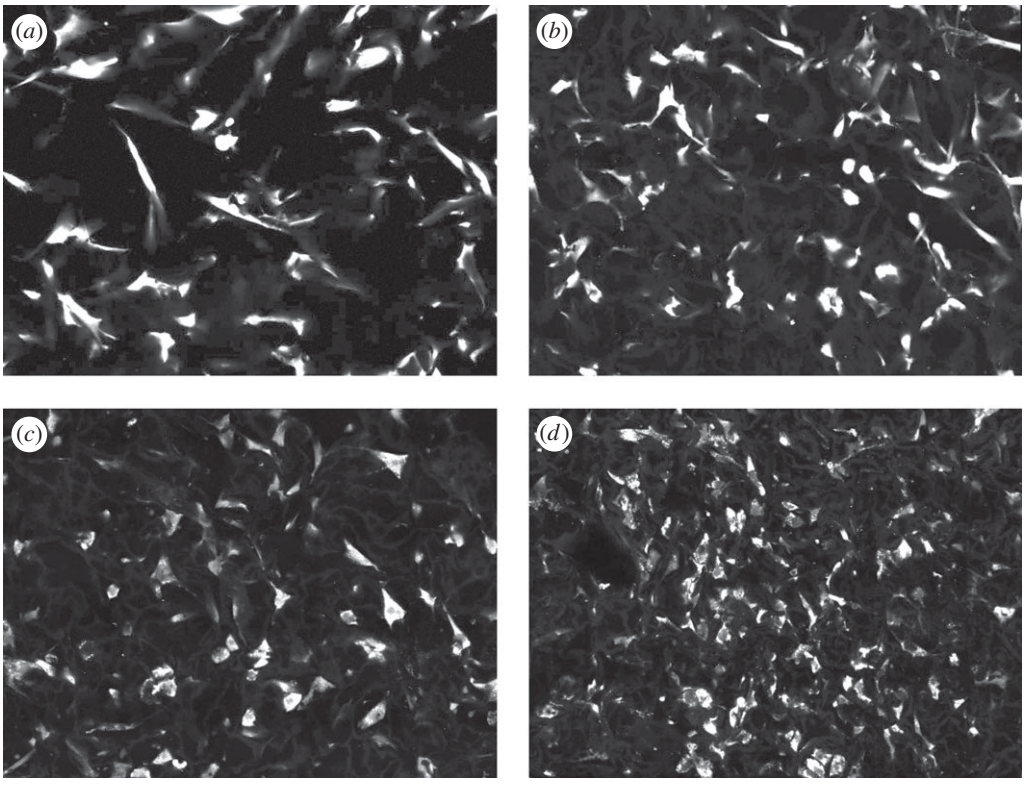

Figure 2. Imaging the differentiation of fibroblasts into myofibroblasts inside CGSs. About 8×10^4 cells were seeded in 8 mm diameter CGSs supplied with complete Dulbecco's modified Eagle medium (DMEM). Starting 24 h after seeding, seeded cells inside the CGS were supplied with complete DMEM containing 1.5 ng ml^{-1} TGFβ1. Fresh medium containing TGFβ1 was applied every 2 days. Four scaffolds were imaged: (*a*) 0 h, (*b*) 1 day, (*c*) 2 days and (*d*) 4 days after starting TGFβ1 treatment. After 7 days of TGFβ1 treatment, the CGS diameter decreased by approximately 50% and expression of α-smooth muscle actin (an established marker for myofibroblast differentiation; Desmouliere *et al.* 2005) was upregulated three-fold compared with basal expression levels. Cells were stained using calcein AM cell tracking dye. All images have 515×386 μm field of view.

Imaging cell–CGS interactions using NLOM offers many advantages compared with alternative three-dimensional methods, such as confocal microscopy. NLOM can image CGS struts based on the SHG emitted by collagen and, therefore, it is not necessary to stain the CGS, avoiding thereby modification of its surface chemistry. The use of infrared lasers and the localized fluorophore excitation around the laser focus result in reduced cellular photodamage, reduced fluorophore photobleaching and the ability to image deeper inside the CGS sample. Studies of cell–matrix interactions can greatly benefit by combining NLOM with genetically encoded fluorescent fusion proteins and smart fluorescent probes (Zhang *et al.* 2002; Lippincott-Schwartz & Patterson 2003). The spatial resolution of NLOM can provide information about the three-dimensional spatial distribution of fluorescently labelled proteins. Advanced imaging modalities such as fluorescent lifetime imaging, fluorescence correlation spectroscopy and Förster

resonance energy transfer can be used to quantify protein–protein interactions, diffusion kinetics and concentration of proteins at intracellular or extracellular locations (Lakowicz 2006).

The authors thank the Dedon lab and the Newman lab, both at MIT, for allowing them to use some of their facilities, Dr A. Roy for his assistance with the fluorescence staining of the fibroblast cells and Prof. R. Hynes for helpful discussions. The study was partially supported by NIH grant no. 5 RO1 NS05320 awarded to I.V.Y.

References

Atala, A. 2005 Regeneration of urologic tissues and organs. *Adv. Biochem. Eng. Biotechnol.* **94**, 179–208. (doi:10.1007/b100004)

Baldwin, C., Potter, M., Clayton, E., Irvine, L. & Dye J. 2009 Topical negative pressure stimulates endothelial migration and proliferation: a suggested mechanism for improved integration of Integra. *Ann. Plast. Surg.* **62**, 92–96. (doi:10.1097/SAP.0b013e31817762fd)

Burke, J. F., Yannas, I. V., Quinby Jr, W. C., Bondoc, C. C. & Jung, W. K. 1981 Successful use of a physiologically acceptable artificial skin in the treatment of extensive burn injury. *Ann. Surg.* **194**, 413–428. (doi:10.1097/00000658-198110000-00005)

Calderwood, D. A., Tuckwell, D. S., Eble, J., Kühn, K. & Humphries, M. J. 1997 The integrin $\alpha 1$ A-domain is a binding site for collagens and laminin. *J. Biol. Chem.* **272**, 12 311–12 317.

Campagnola, P. J. & Loew, L. M. 2003 Second-harmonic imaging microscopy for visualizing biomolecular arrays in cells, tissues and organisms. *Nat. Biotechnol.* **21**, 1356–1360. (doi:10.1038/nbt894)

Chamberlain, L. J., Yannas, I. V., Hsu, H.-P., Strichartz, G. & Spector, M. 1998 Collagen–GAG substrate enhances the quality of nerve regeneration through collagen tubes up to level of autograft. *Exp. Neurol.* **154**, 315–329. (doi:10.1006/exnr.1998.6955)

Chang, A. S. & Yannas, I. V. 1992 Peripheral nerve regeneration. In *Neuroscience year* (eds B. Smith & G. Adelman). Boston, MA: Birkhauser.

Chang, A. S., Yannas, I. V., Perutz, S., Loree, H., Sethi, R. R., Krarup, C., Norregaard, T. V., Zervas, N. T. & Silver, J. 1990 Electrophysiological study of recovery of peripheral nerves regenerated by a collagen–glycosaminoglycan copolymer matrix. In *Progress in biomedical polymers* (ed. C. G. Gebelein). New York, NY: Plenum.

Compton, C. C., Butler, C. E., Yannas, I. V., Warland, G. & Orgill, D. P. 1998 Organized skin structure is regenerated *in vivo* from collagen–GAG matrices seeded with autologous keratinocytes. *J. Invest. Dermatol.* **110**, 908–916. (doi:10.1046/j.1523-1747.1998.00200.x)

Denk, W., Strickler, J. H. & Webb, W. W. 1990 Two-photon laser scanning fluorescent microscopy. *Science* **248**, 73–76. (doi:10.1126/science.2321027)

Desmouliere, A., Chaponnier, C. & Gabbiani, G. 2005 Tissue repair, contraction, and the myofibroblast. *Wound Repair Regen.* **13**, 7–12. (doi:10.1111/j.1067-1927.2005.130102.x.)

Even-Ram, S. & Yamada, K. M. 2005 Cell migration in 3D matrix. *Curr. Opin. Cell Biol.* **17**, 524–532. (doi:10.1016/j.ceb.2005.08.015)

Fang, P. *et al.* 2002 Dermatome setting for autografts to cover INTEGRA(R). *J. Burn Care Rehabil.* **23**, 327–332. (doi:10.1097/01.BCR.0000028567.45444.DF)

Freyman, T. M., Yannas, I. V., Yokoo, R. & Gibson, R. J. 2001 Fibroblast contraction of a collagen–GAG matrix. *Biomaterials* **22**, 2883–2891. (doi:10.1016/S0142-9612(01)00034-5)

Grzesiak, J. J. & Bouvet, M. 2007 Determination of the ligand-binding specificities of the alpha2beta1 and alpha1beta1 integrins in a novel 3-dimensional *in vitro* model of pancreatic cancer. *Pancreas* **34**, 220–228. (doi:10.1097/01.mpa.0000250129.64650.f6)

Harley, B. A., Hastings, A. Z., Yannas, I. V. & Sannino, A. 2006 Fabricating tubular scaffolds with a radial pore size gradient by a spinning technique. *Biomaterials* **27**, 866–874. (doi:10.1016/j.biomaterials.2005.07.012)

Harley, B. A., Leung, J. H., Silva, E. & Gibson, L. J. 2007*a* Mechanical characterization of collagen–glycosaminoglycan scaffolds. *Acta Biomater.* **3**, 463–474. (doi:10.1016/j.aetbio.2006.12.009)

Harley, B. A., Freyman, T. M., Wong, M. Q. & Gibson, L. J. 2007*b* A new technique for calculating individual dermal fibroblast contractile forces generated within collagen–GAG scaffolds. *Biophys. J.* **93**, 2911–2922. (doi:10.1529/biophysj.106.095471)

Harley, B. A., Kim, H. D., Zaman, M. H., Yannas, I. V., Lauffenburger, D. A. & Gibson, L. J. 2008 Microarchitecture of three-dimensional scaffolds influences cell migration behavior via junction interactions. *Biophys. J.* **95**, 4013–4024. (doi:10.1529/biophysj.107.122598)

Harley, B. A., Lynn, A. K., Wissner-Gross, Z., Bonfield, W., Yannas, I. V. & Gibson, L. J. 2009*a* Design of a multiphase osteochondral scaffold. II. Fabrication of a mineralized collagen–glycosaminoglycan scaffold. *J. Biomed. Mater. Res. A* **92A**, 1066–1077. (doi:10.1002/jbm.a.32361)

Harley, B. A., Lynn, A. K., Wissner-Gross, Z., Bonfield, W., Yannas, I. V. & Gibson, L. J. 2009*b* Design of a multi-phase osteochondral scaffold III: fabrication of a mineralized collagen–GAG scaffold. *J. Biomed. Mater. Res. A* **92A**, 1078–1093. (doi:10.1002/jbm.a.32387)

Harley, B. A., Lynn, A. K., Wissner-Gross, Z., Bonfield, W., Yannas, I. V. & Gibson, L. J. 2010 Design and fabrication of a multiphase osteochondral scaffold. II. Fabrication of a mineralized collagen-glycosaminoglycan scaffold. *J. Biomed. Mater. Res. A* **1**, 1066–1077.

Heimbach, D. *et al.* 1988 Artificial dermis for major burns—a multi-center randomized clinical trial. *Ann. Surg.* **208**, 313–320.

Hinz, B. 2006 Masters and servants of the force: the role of matrix adhesions in myofibroblast force perception and transmission. *Eur. J. Cell Biol.* **85**, 175–181. (doi:10.1016/j.ejcb.2005.09.004)

Hsu, W. C., Spilker, M. H., Yannas, I. V. & Rubin, P. A. D. 2000 Inhibition of conjunctival scarring and contraction by a porous collagen–glycosaminoglycan implant. *Invest. Opthamol. Vis. Sci.* **41**, 2404–2411.

Hynes, R. O. 2002 Integrins: bidirectional, allosteric signalling machines. *Cell* **110**, 673–687. (doi:10.1016/S0092-8674(02)00971-6)

Jaworski, J. & Klapperich, C. M. 2006 Fibroblast remodeling activity at two- and three-dimensional collagen–glycosaminoglycan interfaces. *Biomaterials* **27**, 4212–4220. (doi:10.1016/j.biomaterials.2006.03.026)

Kanungo, B. P., Silva, E., Van Vliet, K. & Gibson, L. J. 2008 Characterization of mineralized collagen–glycosaminoglycan scaffolds for bone regeneration. *Acta Biomater.* **4**, 490–503. (doi:10.1016/j.aetbio.2008.01.003)

Katrana, F., Kostopoulos, E., Delia, G., Lunel, G. G. & Casoli, V. 2008 Reanimation of thumb extension after upper extremity degloving injury treated with Integra(R). *J. Hand Surg. Eur. Vol.* **33**, 800–802. (doi:10.1177/1753193408096021)

Kim, J. K., Xu, Y., Xu, X., Keene, D. R., Gurusiddappa, S., Liang, X., Wary, K. S. & Höök, M. 2005 A novel binding site in collagen III for integrins α1β1 and α2β1. *J. Biol. Chem.* **280**, 32 512–32 520.

Kinner, B., Capito, R. M. & Spector, M. 2005 Regeneration of articular cartilage. *Adv. Biochem. Eng. Biotechnol.* **94**, 91–123. (doi:10.1007/b100001)

Klapperich, C. M. & Bertozzi, C. R. 2004 Global gene expression of cells attached to a tissue engineering scaffold. *Biomaterials* **25**, 5631–5641. (doi:10.1016/j.biomaterials.2004.01.025)

Knight, C. G., Morton, L. F., Peachey, A. R., Tuckwell, D. S., Farndale, R. W. & Barnes, M. J. 2000 The collagen-binding A-domains of integrins α1β1 and α2β1 recognize the same specific amino acid sequence, GFOGER, in native (triple-helical) collagens. *J. Biol. Chem.* **275**, 35–40. (doi:10.1074/jbc.275.1.35)

Lakowicz, J. R. 2006 *Principles of fluorescence spectroscopy*, 3rd edn. New York, NY: Springer.

Lippincott-Schwartz, J. & Patterson, G. H. 2003 Development and use of fluorescent protein markers in living cells. *Science* **300**, 87–91. (doi:10.1126/science.1082520)

Lynn, A. K., Best, A. M., Cameron, R. E., Harley, B. A., Yannas, I. V., Gibson, L. J. & Bonfield, W. 2009 Design of a multi-phase osteochondral scaffold I: control of chemical composition. *J. Biomed. Mater. Res. A* **92A**, 1057–1065. (doi:10.1002/jbm.a.32415)

Meshel, A. S., Wei, Q., Adelstein, R. S. & Sheetz, M. P. 2005 Basic mechanism of three-dimensional collagen fibre transport by fibroblasts. *Nat. Cell Biol.* **7**, 157–164. (doi:10.1038/ncb1216)

Mistry, A. S. & Mikos, A. G. 2005 Tissue engineering for bone regeneration. *Adv. Biochem. Eng. Biotechnol.* **94**, 1–22. (doi:10.1007/b99997)

Murphy, G. F., Orgill, D. P. & Yannas, I. V. 1990 Partial dermal regeneration is induced by biodegradable collagen–glycosaminoglycan grafts. *Lab. Invest.* **62**, 305–313.

O'Brien, F. J., Harley, B. A., Yannas, I. V. & Gibson, L. J. 2004 Influence of freezing rate on pore structure in freeze-dried collagen–GAG scaffolds. *Biomaterials* **25**, 1077–1086. (doi:10.1016/S0142-9612(03)00630-6)

O'Brien, F. J., Harley, B. A., Yannas, I. V. & Gibson, L. J. 2005 The effect of pore size on cell adhesion in collagen–GAG scaffolds. *Biomaterials* **26**, 433–441. (doi:10.1016/j.biomaterials.2004.02.052)

Orgill, D. P. & Yannas, I. V. 1998 Design of an artificial skin. IV. Use of island graft to isolate organ regeneration from scar synthesis and other processes leading to skin wound closure. *J. Biomed. Mater. Res.* **36**, 531–535. (doi:10.1002/(SICI)1097-4636(19980315)39:4<531::AID-JBM4>3.0.CO;2-K)

Park, H., Cannizzaro, C., Vunjak-Novakovic, G., Langer, R., Vacanti, C. A. & Farokhzad, O. C. 2007 Nanofabrication and microfabrication of functional materials for tissue engineering. *Tissue Eng.* **13**, 1867–1877. (doi:10.1089/ten.2006.0198)

Pek, Y.S., Spector, M., Yannas, I. V. & Gibson, L. J. 2004 Degradation of a collagenchondroitin-6-sulfate matrix by collagenase and by chondroitinase. *Biomaterials* **25**, 473–482. (doi:10.1016/S0142-9612(03)00541-6)

Rabkin-Aikawa, E., Mayer, J. E. & Schoen, F. J. 2005 Heart valve regeneration. *Adv. Biochem. Eng. Biotechnol.* **94**, 141–178. (doi:10.1007/b100003)

Racine-Samson, L., Rockey, D. C. & Bissell, D. M. 1997 The role of alpha 1 beta 1 integrin in wound contraction. A quantitative analysis of liver myofibroblasts *in vivo* and in primary culture. *J. Biol. Chem.* **272**, 30 911–30 917.

Ridley, A. J., Schwartz, M. A., Burridge, K., Firtel, R. A., Ginsberg, M. H., Borisy, G., Parsons, J. T. & Horwitz, A. R. 2003 Cell migration: integrating signals from front to back. *Science* **302**, 1704–1709. (doi:10.1126/science.1092053)

Sasidaran, R., Dorai, A. A., Sulaiman, W. A. & Halim, A. S. 2008 Use of dermal regeneration template (INTEGRA) in reconstructive burn surgery. *Med. J. Malaysia* **63**(Suppl. A), 29.

So, P.T.C., Dong, C. Y., Masters, B. R. & Berland, K. M. 2000 Two-photon excitation fluorescence microscopy. *Annu. Rev. Biomed. Eng.* **2**, 399–429. (doi:10.1146/annurev.bioeng.2.1.399)

Sylvester, M. F., Yannas, I. V., Salzman, E. W. & Forbes, M. J. 1989 Collagen banded fibril structure and the collagen-platelet reaction. *Thromb. Res.* **55**, 135–148. (doi:10.1016/0049-3848(89)90463-5)

Timmins, N. E., Scherberich, A., Früh, J. A., Heberer, M., Martin, I. & Jakob, M. 2007 Three-dimensional cell culture and tissue engineering in a T-CUP (tissue culture under perfusion). *Tissue Eng.* **13**, 2021–2028. (doi:10.1089/ten.2006.0158)

Tuckwell, D., Calderwood, D. A., Green, L. J. & Humphries, M. J. 1995 Integrin alpha-2 I-domain is a binding site for collagens. *J. Cell Sci.* **108**, 1629–1637.

Tulla, M., Pentikäinen, O. T., Viitasalo, T., Käpylä, J., Impola, U., Nykvist, P., Nissinen, L., Johnson, M. S. & Heino, J. 2001 Selective binding of collagen subtypes by integrin α1I, α2I, and α10I domains. *J. Biol. Chem.* **276**, 48 206–48 212.

Verma, P. & Fawcett, J. 2005 Spinal cord regeneration. *Adv. Biochem. Eng. Biotechnol.* **94**, 43–66. (doi:10.1007/b99999)

Wakabayashi, T. *et al.* 2008 A multicenter phase I trial of interferon-beta and temozolomide combination therapy for high-grade gliomas (INTEGRA Study). *Jpn. J. Clin. Oncol.* **38**, 715–718. (doi:10.1093/jjco/hyn095)

Yamada, K. M. & Cukierman, E. 2007 Modeling tissue morphogenesis and cancer in 3D. *Cell* **130**, 601–610. (doi:10.1016/j.cell.2007.08.006)

Yannas, I. V. 1990 Biologically active analogs of the extracellular matrix. *Angew. Chem. Engl. Ed.* **29**, 20–35.

Yannas, I. V. 2001 *Tissue and organ regeneration in adults.* New York, NY: Springer.

Yannas, I. V. (ed.) 2005*a* *Regenerative medicine*, vol. 2. Heidelberg, Germany: Springer.

Yannas, I. V. 2005*b* Similarities and differences between induced organ regeneration in adults and early fetal regeneration. *J. R. Soc. Interface* **2**, 403–417. (doi:10.1098/rsif.2005.0062)

Yannas, I. V. 2005*c* Facts and theories of organ regeneration. *Adv. Biochem. Eng. Biotechnol.* **93**, 1–31. (doi:10.1007/b99965)

Yannas, I. V., Burke, J. F., Gordon, P. L., Huang, C. & Rubenstein, R. H. 1980 Design of an artificial skin. II. Control of chemical composition. *J. Biomed. Mater. Res.* **14**, 107–131. (doi:10.1002/jbm.820140203)

Yannas, I. V., Burke, J. F., Warpehoski, M., Stasikelis, P., Skrabut, E. M., Orgill, D. & Giard, D. J. 1981 Prompt, long-term functional replacement of skin. *Trans. Am. Soc. Artif. Intern. Organs* **27**, 19–22.

Yannas, I. V., Burke, J. F., Orgill, D. P. & Skrabut, E. M. 1982 Wound tissue can utilize a polymeric template to synthesize a functional extension of skin. *Science* **215**, 174–176. (doi:10.1126/science.7031899)

Yannas, I. V., Lee, E., Orgill, D. P., Skrabut, E. M. & Murphy, G. F. 1989 Synthesis and characterization of a model extracellular-matrix that induces partial regeneration of adult mammalian skin. *Proc. Natl Acad. Sci. USA* **86**, 933–937. (doi:10.1073/pnas.86.3.933)

Yannas, I. V., Gibson, L. J., O'Brien, F. J., Harley, B., Brau, R. R., Samouhos, S. & Spector, M. 2006 *Gradient scaffolding and methods of producing the same*. US patent application 2006/0121609 A1.

Zhang, M. & Yannas, I. V. 2005 Peripheral nerve regeneration. *Adv. Biochem. Eng. Biotechnol.* **94**, 67–89. (doi:10.1007/b100000)

Zhang, J., Campbell, R. E., Ting, A. Y. & Tsien, R. Y. 2002 Creating new fluorescent probes for cell biology. *Nat. Rev. Mol. Cell Biol.* **3**, 906–918. (doi:10.1038/nrm976)

Zipfel, W. R., Williams, R. M. & Webb, W. W. 2003 Nonlinear magic: multiphoton microscopy in the biosciences. *Nat. Biotechnol.* **21**, 1369–1377. (doi:10.1038/nbt899)